COMMUNICATION

# Synthesis of dense porous layered double hydroxides from struvite†

W. L. Joyce Kwok, [ID] Hongri Suo, Chunping Chen, D. W. Justin Leung, Jean-Charles Buffet [ID] and Dermot O'Hare [ID] *

We report an atom economic synthesis of a new type of dense porous layered double hydroxides (SLDHs) using struvite which is a commonly produced undesirable waste in wastewater treatment plants. The obtained SLDHs exhibit significantly higher specific surface areas and larger pore volumes than conventional coprecipitated LDHs but retain a comparable particle density.

Layered double hydroxides (LDHs) are a class of 2D layered materials with the general formula $[(M_{1-x}^{z+}M'_x{}^{y+}(OH)_2)]^{w+}(A^{n-})_{w/n}\cdot mH_2O]$, where M and M' are typically di- or trivalent cations, respectively; and A is an n-valent anionic moiety, either organic or inorganic. The overall metal hydroxide layer charge (w) is controlled by $w = z(1-x) + xy - 2$ which is compensated by w/n A^{n-} interlayer anions.[1] Owing to their distinguished properties such as compositional flexibility, biocompatibility, acid/base tunability and anion exchangeability, LDHs have garnered increasing attention across a wide range of fields (*e.g.*: catalysis, biology, environment and energy) for both fundamental research and commercial applications.[2–6] LDHs are commonly synthesised at scale using metal salts, such as nitrates and chlorides,[7] or oxides.[8,9] There continues to be scope for both increasing the atom efficiency of LDH syntheses and utilising resources in a circular economic way. For example, at an commercial-scale LDH plant in Dalian (China), magnesium aluminium LDHs were prepared using magnesium chloride ($MgCl_2$) from the bitterns remaining after the crystallisation of sodium and potassium chloride from seawater.[7]

Struvite ($MgNH_4PO_4\cdot6H_2O$) is a naturally occurring orthophosphate mineral that precipitates in aqueous systems containing high concentrations of ammonium and phosphate. It was first identified in wastewater treatment plants (WWTPs) in the late 1930s.[10] It can precipitate spontaneously in some

Chemistry Research Laboratory, Department of Chemistry, University of Oxford, 12 Mansfield Road, Oxford, OX1 3TA, UK. E-mail: dermot.ohare@chem.ox.ac.uk

†Electronic supplementary information (ESI) available: Powder XRD, ICP-MS, TGA, FTIR, solid state NMR spectroscopy, BET, BJH and HR-SEM. See DOI: 10.1039/d0gc04410e

areas of WWTPs where the pH, temperature, and magnesium/phosphorus/ammonium ion concentrations are suitable.[11] Struvite is sparingly soluble in water (169.2 mg cm^{-3} at 25 °C)[12] and so creates significant problems for WWTPs, it easily forms hard crystalline deposits that lead to pipeline blockages, resulting in costly and time consuming cleaning and maintenance.[10] The intentional and controlled precipitation of struvite in a dedicated vessel can be deployed by regulating the concentrations of Mg^{2+}, PO_4^{3-} and NH_4^+ (eqn (1)).[13]

$$Mg^{2+} + NH_4^+ + H_nPO_4^{(3-n)-} + 6H_2O \rightarrow MgNH_4PO_4\cdot6H_2O + nH^+ \tag{1}$$
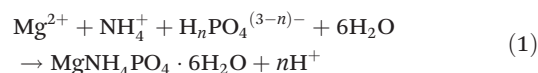
This approach can effectively alleviate pipeline blockages, but it results in the annual production of large quantities of struvite solid discharge from WWTPs. It is of significant importance to develop new efficient circular economic approaches to reuse this waste mineral resource. The low solubility and high nutrient content (magnesium/phosphorus/nitrogen) of struvite make it a potential slow-release fertiliser for agricultural use.[14] However, there are some concerns that the struvite sourced from WWTPs present a potential health risk and as a result is not certified as end-of-waste in many countries.[15,16] Its application as a fertiliser is currently limited by local policy. Therefore, the development of alternative uses of this material is desirable in order to reduce the cost of waste disposal and to increase the efficiency of our chemical processes.

Herein, we explore struvite as a low-cost starting material to synthesise novel morphology magnesium aluminium LDHs using a bespoke *in situ* solid–solid growth method. This method has the advantage over traditional route of LDH synthesis of reducing the amount of waste from water treatment plant, the use of expensive magnesium salts and the production of salt-rich effluent streams that are harmful to the environment.[17]

Although struvite can be used directly to make LDHs we have determined that a pre-treatment step significantly improves the efficiency of the process. Struvite is initially sus-

pended in aqueous sodium hydroxide (1 M) at 85 °C for 1 hour. Ammonia is liberated that can be collected using a HCl trap to yield NH_4Cl, an additional valuable by-product. To obtain phase pure struvite-derived $[Mg_{0.75}Al_{0.25}(OH)_2](CO_3)_{0.175}$ (Mg_3Al-CO_3 SLDH) sodium carbonate and aluminium nitrate are then introduced and this suspension is maintained at pH 11.5, 85 °C for 2 hours (by addition of NaOH). We do not observe dissolution of the mineral precursor; imaging the particles before and after synthesis (*vide infra*) suggest that it may be a solid–solid transformation. The struvite starting material is highly crystalline with an orthorhombic unit cell containing hydrogen-bonded PO_4^{3-} tetrahedra, NH_4^+ tetrahedra and distorted $Mg(H_2O)_6^{2+}$ octahedra (Fig. 1a).[11] After the synthesis reaction, filtration and drying the XRD pattern of the isolated solid is shown in Fig. 1b. The Bragg reflections observed in the XRD can indexed to 00*l*, 01*l*, 11*l*, corresponding to unit cell dimensions of Mg_3Al-CO_3 SLDH, no other crystalline phases are observed.

Thermogravimetric analysis (TGA) of struvite (Fig. S1†) exhibits one main weight loss (approximately 45% of its mass) before 150 °C, which is attributed to the liberation of ammonia and surface water. Further heating causes the loss of structural water and the formation of magnesium phosphates.[18] At 800 °C, the material has lost around 55% of its original mass. In comparison, the Mg_3Al-CO_3 SLDH presents the archetypical thermal decomposition profile of an LDH:[19] loss of surface and interlayer water (17.5 wt%) below 200 °C, followed by dehydroxylation and loss of interlayer carbonate as CO_2 above 200 °C, leading a total loss of 44.3 wt% at 800 °C.

A series of further spectroscopic studies were carried out in order to fully understand the conversion process and the nature of the Mg_3Al-CO_3 SLDH product. Fourier-transform infrared (FTIR) spectra are shown in Fig. S2,† four main band regions are observed for struvite (Fig. S2a†). The broad bands

in the range 2550–3300 cm^{-1} are assigned to the antisymmetric stretching vibration of NH_4 and the OH stretching mode of H_2O. The weak band between 2200–2500 cm^{-1} is due to hydrogen bonding between H_2O and PO_4. The bands between 1300–1800 cm^{-1} are ascribed to the deformations of H–O–H and H–N–H. Strong PO_4^{3-} vibration bands can be observed around 1000 cm^{-1}.[20] After the synthesis reaction, vibrational bands characteristic of LDH can be clearly observed (Fig. S2b†): 3200–3700 cm^{-1} (OH^- and H_2O hydrogen bonding), 1364 cm^{-1} (ν_4/ν_2 vibrations of CO_3^{2-}) and 600–1100 cm^{-1} (O–M–O bending/stretching/deformation), indicating the successful formation of an LDH.[21] In addition, all vibrations due to NH_4^+ were absent, confirming that ammonia had been liberated during the synthesis. Vibrations due to phosphate ions were much weaker in the final LDH product, indicating phosphate is not the main interlayer anion within the interlayer galleries. However, a small amount of PO_4^{3-} remains in the Mg_3Al-CO_3 SLDH, which can be detected by solid state ^{31}P NMR spectroscopy (Fig. S3†) and ICP-MS (Table S1†). The total phosphorus content in the sample was typically 1.4 wt%. The ICP-MS data indicates that the Mg : Al ratio in the SLDH is 2.99, which is close to the theoretical value (3), indicating the magnesium has been fully incorporated in Mg_3Al-CO_3 SLDH. Powder XRD diffractograms of carbonate and phosphate SLDHs for two different Mg/Al ratios (Fig. S4†) and their corresponding *d*-spacing (Table S2†) show the expected 00*l* and interlayer distances.

The morphologies of the materials before and after the synthesis reaction have been investigated using scanning electron microscopy (SEM) and transmission electron microscopy (TEM). As shown in Fig. 2a, struvite presents as coffin-shaped prismatic crystals with dimensional ranges 20–80 μm × 10–20 μm. The SEM images reveal the surface of the struvite crystals are stone-like and smooth (Fig. 2b). After the reaction, the isolated material retains a large particle morphology, but the surface of the particles is now much rougher with small particles observed on the surface (Fig. 2c). TEM imaging after
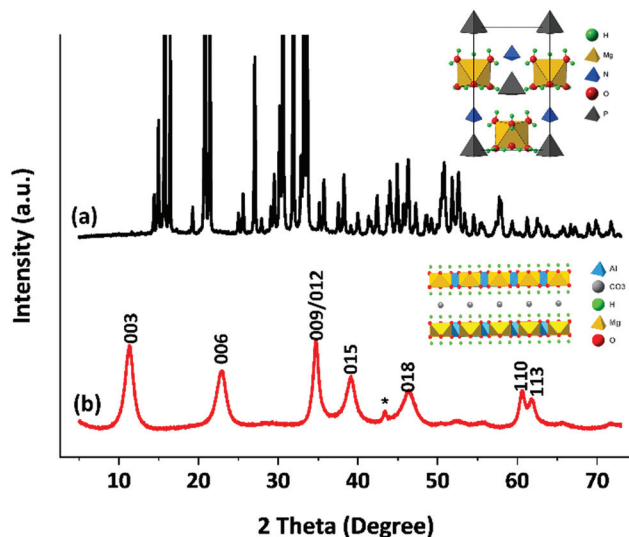

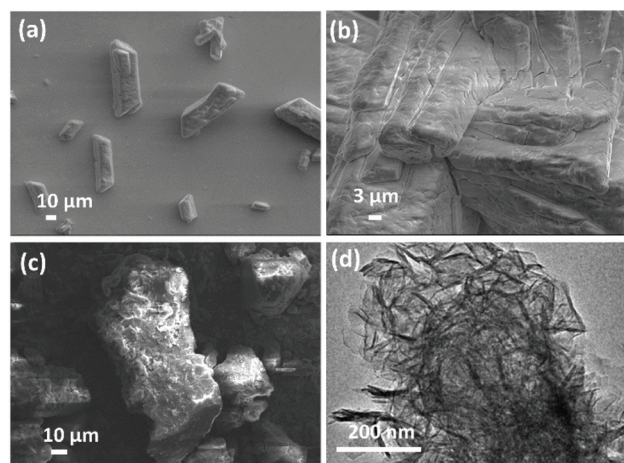**Fig. 1** Powder XRD diffractograms of (a) struvite and (b) Mg_3Al-CO_3 SLDH. *Bragg reflection due to the sample holder.

Fig. 2 SEM images of (a) and (b) struvite, (c) Mg_3Al-CO_3 SLDH, and TEM image of (d) Mg_3Al-CO_3 SLDH.

sonication of these particles in ethanol reveals a classical rosette shape clusters that are composed of primary LDH nanosheets (Fig. 2d).

To better understand the formation process of Mg_3Al-CO_3 SLDH from struvite, we first isolated the material following pre-treatment of struvite in sodium hydroxide at 85 °C for 1 hour. The high resolution (HR) SEM and energy dispersive X-ray (EDX) reveal that the original coffin-lid crystals become cracked and fragmented (Fig. S6†). Sodium, magnesium and phosphorus are uniformly distributed over these particles, which suggests the formation of a metastable intermediate in which the ammonium ions within the original struvite structure are replaced by smaller sodium cations (eqn (2)).

$$MgNH_4PO_4 \cdot 6H_2O + NaOH$$
$$\rightarrow MgNaPO_4 \cdot 6H_2O + NH_3 + H_2O \quad (2)$$
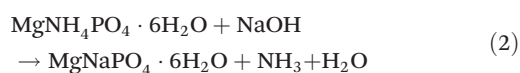
ICP-MS data of this material has a $Mg:Na:P$ ratio of $2:1:2$ indicating partial exchange of the ammonium cations (Table S3†).

Hence, we postulate that Mg_3Al-CO_3 SLDH formation proceeds *via* a reactive intermediate that is unique to the synthesis route. The struvite-like structure of proposed "$MgNa_x(NH_4)_yPO_4\cdot6H_2O$" ($MgNa_{0.5}(NH_4)_{0.5}PO_4\cdot6H_2O$ according to the ICP-MS data in this case) material provides a framework to grow Mg_3Al-CO_3 SLDH nanosheets. Nucleation and growth of the Mg_3Al-CO_3 SLDH proceeds directly on the surface of this intermediate *via* a dissolution-crystallisation process, giving rise to a struvite-like porous framework composed of hierarchical LDH rosettes. This is confirmed by characterisation by powder XRD, solid state NMR spectroscopy and specific surface area and pore volume measurements (Fig. S7–S11†).

We ascribe this dissolution-crystallisation process on the surface of the intermediate magnesium phosphate as the origin of the unique porosity of Mg_3Al-CO_3 SLDH. The specific surface area and pore volume of Mg_3Al-CO_3 SLDH as measured by N_2 BET measurements are 184 m^2 g^{-1} and 0.75 cm^3 g^{-1}, respectively (Fig. 3 and S5†). These values are significantly higher than conventional water-washed Mg_3Al-CO_3 LDH (43 m^2 g^{-1} and 0.11 cm^3 g^{-1}) synthesised by traditional co-precipitation methods.[22] In fact, these porosity figures resemble those obtained in the aqueous miscible organic solvent treatment method (AMOST) to yield AMO-Mg_3Al-CO_3 LDH (212 m^2 g^{-1} and 0.75 cm^3 g^{-1}).[22–24] Fig. S5† also shows the different shapes of N_2 adsorption/desorption isotherms of SLDH and AMO-SLDH above $P/P_0 = 0.7$ which suggests different origins of the porosity. It is likely inter-particle porosity for AMO-SLDH with straight and parallel adsorption and desorption branches until higher adsorbed N_2 volume while the hysteresis loop suggests intra-particle porosity SLDH. AMO-LDHs with high specific surface area typically possess very low powder densities (tap density *ca.* 0.2 g cm^{-3}),[22] this feature can create some powder handling challenges especially during large scale production. Interestingly, the Mg_3Al-CO_3 SLDH developed in this study exhibits not only high surface area and pore volume, but also relatively high particle density (tap density = 0.64 g
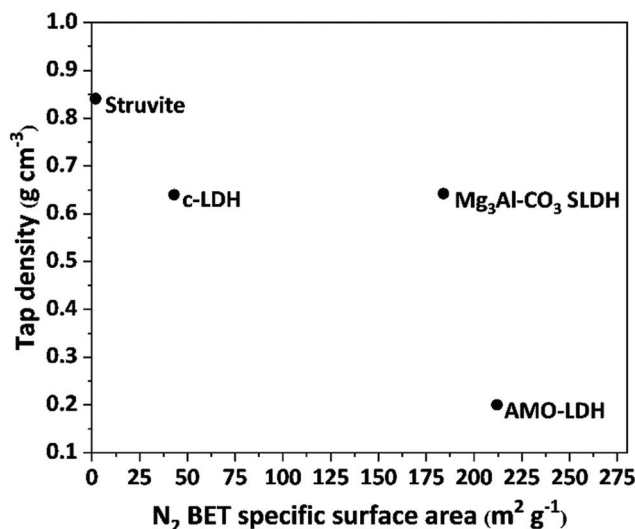

Fig. 3 N_2 BET specific surface areas and powder tap densities of different materials. The c-LDH is a conventional water-washed Mg_3Al-CO_3 LDH. The AMO-LDH is an Mg_3Al-CO_3 LDH post synthesis dispersed in acetone.[22]

cm^{-3}) which is three times higher than that of a typical AMO-LDH. We concluded that the high surface area and pore volume created in Mg_3Al-CO_3 SLDH is derived by the internal void structure of the aggregated SLDH particles that is a direct consequence of using a struvite-derived precursor during synthesis.

We have also prepared porous Mg_2Al-CO_3 SLDH by adjusting the ratio of struvite to aluminium nitrate (Fig. S4†). By omitting the Na_2CO_3 in the synthesis and operating under a nitrogen atmosphere we can utilise the phosphate anions within the struvite to make Mg_nAl-PO_4 SLDH ($n = 2, 3$) (Fig. S4†). We observe a slight increase in the interlayer separation from 7.78 Å to 7.93 Å between Mg_3Al-CO_3 SLDH and Mg_3Al-PO_4 SLDH (Table S2†). We have also carried out SLDH synthesis using two commercial waste water treatment plant (WWTP) struvite samples (Table S4, Fig. S13†). Although technologies used to precipitate these commercial struvites differ and as a result the composition and morphology (Fig. S14–S17†) of the struvite samples differ from that observed of the pure struvite purchased from Alfa Aesar both produced SLDHs with excellent yield and purity. Some differences in pore volume were observed (Fig. S18†).

We believe that this new class of dense and porous SLDH will be an attractive material in many applications such as heterogeneous catalysis, adsorption, and energy storage. Therefore we have performed some preliminary studies on carbon dioxide (CO_2) capture to demonstrate that an LDH derived from struvite waste could be a promising candidate as a low-cost, efficient carbon capture material. It is well known that LDHs can be transformed into uniquely structured mixed metal oxides (LDOs) by calcination at temperatures in the range 300–550 °C.[25,26] Calcination of Mg_3Al-CO_3 SLDH above 400 °C produces an SLDO which shows a complex aluminium/magnesium phase that possess both basicity and acidity in the
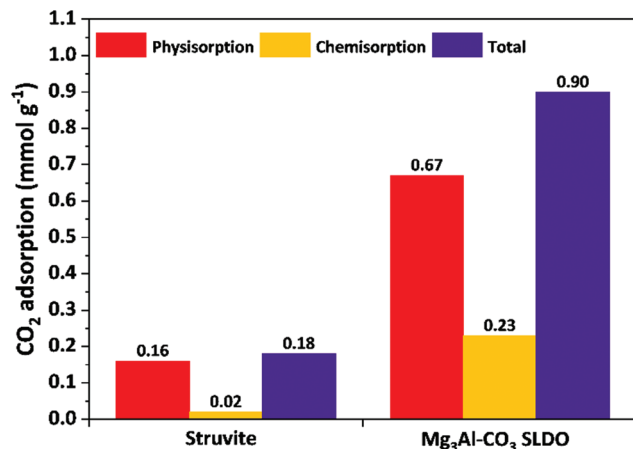
Fig. 4 CO_2 adsorption of struvite and Mg_3Al-CO_3 SLDO at 40 °C and 100 kPa. The samples were initially calcined at 400 °C for 2 hours.

medium-high strength range (Fig. S19†).[27–29] In addition, the specific surface area (Fig. S20†) and pore volume (Fig. S21†) further increases up to 203 m² g⁻¹ and 0.84 cm³ g⁻¹, respectively, when it is calcined at 400 °C for 2 hours. All these materials features are particularly appropriate for the adsorption of CO_2.

Fig. 4 shows the CO_2 adsorption performances of struvite and SLDO. Struvite exhibits poor CO_2 adsorption capacity (0.18 mmol g⁻¹ at 40 °C and 100 kPa), which includes 0.16 mmol g⁻¹ of physisorption and 0.02 mmol g⁻¹ of chemisorption. This is mainly due to its low specific surface area and almost no active sites for CO_2 adsorption. In contrast, the CO_2 adsorption capability of Mg_3Al-CO_3 SLDH is 0.9 mmol g⁻¹, four times higher than that of struvite, 74% of this capacity is due to physisorption, which is ascribed to high specific surface area and large pore volume, whilst 26% is chemisorption that is ascribed to the presence of moderate basic sites in the SLDO.[28,30]

In summary, we have shown that struvite (including waste water treatment plant samples) can be both an efficient, green source of magnesium and phosphate and create a structural scaffold for the preparation of a new class of dense porous Mg_nAl-A SLDHs (n = 2, 3; A = CO_3, PO_4). Our preliminary studies suggest the transformation proceeds via a dissolution-crystallisation mechanism; possesses high surface area, large pore volume and high tap densities, a combination not found in conventional LDHs and AMO-LDHs.

Additionally, the SLDO derived from Mg_3Al-CO_3 SLDH exhibits four times higher CO_2 adsorption than that of struvite. These findings demonstrate that the synthesis in this study can upgrade the struvite mineral into valuable LDH-based materials.

Conflicts of interest

There are no conflicts to declare.

References

1 *Layered Double Hydroxides*, ed. X. Duan and D. G. Evans, Springer-Verlag Berlin Heidelberg, 2005.
2 S. Miyata, *Clays Clay Miner.*, 1983, **31**, 305–311.
3 A. I. Khan, A. Ragavan, B. Fong, C. Markland, M. O'Brien, T. G. Dunbar, G. R. Williams and D. O'Hare, *Ind. Eng. Chem. Res.*, 2009, **48**, 10196–10205.
4 G. Fan, F. Li, D. G. Evans and X. Duan, *Chem. Soc. Rev.*, 2014, **43**, 7040–7066.
5 S. He, Z. An, M. Wei, D. G. Evans and X. Duan, *Chem. Commun.*, 2013, **49**, 5912–5920.
6 Z. Cao, B. Li, L. Sun, L. Li, Z. P. Xu and Z. Gu, *Small Methods*, 2020, **4**, 1900343.
7 D. G. Evans and X. Duan, *Chem. Commun.*, 2006, 485–496.
8 S. P. Newman, W. Jones, P. O'Connor and D. N. Stamires, *J. Mater. Chem.*, 2002, **12**, 153–155.
9 Z. P. Xu and G. Q. Lu, *Chem. Mater.*, 2005, **17**, 1055–1062.
10 Y. Jaffer, T. A. Clark, P. Pearce and S. A. Parsons, *Water Res.*, 2002, **36**, 1834–1842.
11 K. S. Le Corre, E. Valsami-Jones, P. Hobbs and S. A. Parsons, *Crit. Rev. Environ. Sci. Technol.*, 2009, **39**, 433–477.
12 M. I. H. Bhuiyan, D. S. Mavinic and R. D. Beckie, *Environ. Technol.*, 2007, **28**, 1015–1026.
13 S. Kataki, H. West, M. Clarke and D. C. Baruah, *Resour., Conserv. Recycl.*, 2016, **107**, 142–156.
14 H. D. Ryu, C. S. Lim, M. K. Kang and S. I. Lee, *J. Hazard. Mater.*, 2012, **221**, 248–255.
15 Q.-L. Chen, X.-L. An, Y.-G. Zhu, J.-Q. Su, M. R. Gillings, Z.-L. Ye and L. Cui, *Environ. Sci. Technol.*, 2017, **51**, 8149–8157.
16 M. Otoo, P. Drechsel, *Resource recovery from waste: business models for energy, nutrient and water reuse in low- and middle-income countries*, Routledge - Earthscan, Oxon, UK, 2018, pp. 316–546.
17 F. J. W. J. Labuschagné, A. Wiid, H. P. Venter, B. R. Gevers and A. Leuteritz, *Green Chem. Lett. Rev.*, 2018, **11**, 18–28.
18 M. I. H. Bhuiyan, D. Mavinic and F. Koch, *Chemosphere*, 2008, **70**, 1347–1356.
19 W. Yang, Y. Kim, P. K. T. Liu, M. Sahimi and T. T. Tsotsis, *Chem. Eng. Sci.*, 2002, **57**, 2945–2953.
20 G. Kurtulus and A. Tas, *Mater. Lett.*, 2011, **65**, 2883–2886.
21 C. Chen, K. Ruengkajorn, J.-C. Buffet and D. O'Hare, *RSC Adv.*, 2018, **8**, 34650–34655.
22 C. Chen, M. Yang, Q. Wang, J.-C. Buffet and D. O'Hare, *J. Mater. Chem. A*, 2014, **2**, 15102–15110.

23 Q. Wang and D. O'Hare, *Chem. Commun.*, 2013, **49**, 6301–6303.

24 C. Chen, A. Wangriya, J.-C. Buffet and D. O'Hare, *Dalton Trans.*, 2015, **44**, 16392–16398.

25 M. A. Aramendía, Y. Avilés, V. Borau, J. M. Luque, J. M. Marinas, J. R. Ruiz and F. J. Urbano, *J. Mater. Chem.*, 1999, **9**, 1603–1607.

26 F. Rey, V. Fornés and J. M. Rojo, *J. Chem. Soc., Faraday Trans.*, 1992, **88**, 2233–2238.

27 Y. Gao, Z. Zhang, J. Wu, X. Yi, A. Zheng, A. Umar, D. O'Hare and Q. Wang, *J. Mater. Chem. A*, 2013, **1**, 12782–12790.

28 D. W. J. Leung, C. Chen, J.-C. Buffet and D. O'Hares, *Dalton Trans.*, 2020, **49**, 9306–9311.

29 F. Prinetto, G. Ghiotti, R. Durand and D. Tichit, *J. Phys. Chem. B*, 2000, **104**, 11117–11126.

30 X. Zhu, C. Chen, H. Suo, Q. Wang, Y. Shi, D. O'Hare and N. Cai, *Energy*, 2019, **167**, 960–969.